Soft Matter

PAPER

View Article Online
View Journal | View Issue

Cite this: *Soft Matter*, 2022, **18**, 6200

Experimental investigation of anomalous molecular probe diffusion in entangled polymer melts†

D. Nieto Simavilla, ‡[a] V. Ramakrishnan, ‡[b] S. K. Smoukov‡[c] and D. C. Venerus ‡*[d]

Investigations on the diffusion of small molecules or particles in polymeric materials are important to numerous technologies and can also be used to gain insight on polymer chain dynamics. Systems where the probe size is comparable to (or smaller than) a characteristic length of the polymer chain, the tube diameter for example, are of particular interest because the diffusion coefficient of the probe can be orders of magnitude larger than the value predicted by the Stokes–Einstein relation. In the present study, we employ the optical technique known as forced Rayleigh scattering to study the diffusion of a molecular probe (dye) in several entangled polymer melts over a wide range of length and time scales. The probe size is much smaller than the tube diameter for the systems studied. We find the diffusion coefficient is larger by four to five orders of magnitude than the Stokes–Einstein prediction. More interestingly, we observe anomalous, non-Fickian, diffusion where the value of the measured diffusion coefficient can abruptly change by as much as 50%. We suggest that this unexpected behavior occurs when the time scale for diffusion is larger than the relaxation time associated with the constraint release mechanism for polymer chain dynamics.

Received 8th June 2022,
Accepted 16th July 2022

DOI: 10.1039/d2sm00759b

rsc.li/soft-matter-journal

1 Introduction

The diffusion of small molecules or particles in polymeric materials is important to numerous technologies.[1] For example, diffusive transport occurs in polymer synthesis and processing, and is critical to the performance of packaging materials, membranes, drug delivery systems. The diffusion of small probes, either molecular or nanoparticle, can also be used to gain insight on polymer chain dynamics.

In a low-molecular weight liquid (solvent), the diffusion of small molecules or colloidal particles (solute) is well understood. For such systems, the translational motion of the solute is governed by the balance between the thermal energy (collisions) and viscous forces (drag) due to solvent molecules. This balance results in the mean-square displacement of the solute having a linear dependence on time, or so-called Fickian diffusion. As a result, the diffusion coefficient D can be estimated[2] using the celebrated Stokes–Einstein equation:

$$D = \frac{k_B T}{6\pi\eta R}, \quad (1)$$

where η is viscosity of the solvent, R is the (effective) radius of the spherical solute, and k_B is the Boltzmann constant.

It is less clear that the Stokes–Einstein eqn (1) is valid for the diffusion of small molecules or particles in polymeric materials. For example, the diffusion of molecular probes (dyes) in polymers near the glass transition temperature show deviations from (1) that can be several orders of magnitude.[3,4] More recently, the diffusion of nanoparticles in polymers has received considerable attention.[5,6] The diffusion coefficient D for such systems shows a strong dependence on the size of the nanoparticle $2R$ relative to the Edwards polymer tube diameter a, which has values $a \sim$ 5–10 nm for entangled polymer melts. For $2R/a \gg 1$, the diffusion coefficient follows the prediction of (1). This indicates nanoparticle diffusion is coupled to the dynamics of entangled polymer chains, which have well-known dependencies on temperature and molecular weight. However, for systems where $2R/a \sim 1$ both experiments[7–10] and theoretical predictions[11,12] indicate that D has a strong dependence on $2R/a$ with values that can be several orders of magnitude larger

[a] *Basque Center for Applied Mathematics, 48009 Bilbao, Bizkaia (Basque-Country), Spain*
[b] *SABIC, Plasticslaan 1, 4612PX Bergen op Zoom, The Netherlands*
[c] *School of Engineering and Materials Science, Queen Mary University of London, London E1 4NS, UK*
[d] *Department of Chemical & Materials Engineering, New Jersey Institute of Technology, Newark, NJ 01072, USA. E-mail: venerus@njit.edu*

† Dedicated to Professor James S. Vrentas of Penn State University whose seminal research on diffusion in polymers was the inspiration for this study.

‡ This work was performed while the authors were in the Department of Chemical & Biological Engineering, Illinois Institute of Technology, Chicago, IL 60616, USA.

than predicted by (1). For systems with $2R/a \lessapprox 1$, nanoparticle diffusion is decoupled from the polymer chain dynamics and the particle experiences a dramatically reduced viscous drag from the polymer chain segments that surround it.

Diffusion coefficients of small molecules and particles in polymers can be 10 orders of magnitude smaller than those in ordinary, low-molecular weight, liquids. Consequently, a number of optical techniques have been developed that probe smaller length scales and therefore allow for the measurement of D in polymeric materials. These techniques include fluorescence correlation spectroscopy (FCS),[9,13–15] photon correlation spectroscopy (PCS),[16] fluorescence recovery after photo bleaching (FRAP),[17,18] and forced Rayleigh scattering (FRS).[19–25] Each of these techniques have their (dis)advantages, and typically the length scale for the diffusion measurements is varied by less than a factor of 10.

For two-component ideal mixtures, mass diffusion typically is assumed to be governed by Fick's law. For constant density systems, Fick's law for the diffusive mass flux of species A can be written as

$$j_A = -D\nabla\rho_A, \tag{2}$$

where ρ_A is the mass density of species A and D is the (binary) diffusion coefficient. Substitution of (2) in the species A mass balance that governs $\rho_A(x, t)$ leads to the diffusion equation

$$\frac{\partial\rho_A}{\partial t} = \frac{\partial}{\partial x}\left(D\frac{\partial\rho_A}{\partial x}\right). \tag{3}$$

Studies of diffusion in polymeric systems often use solutions of (3) subject to appropriate initial and boundary conditions to interpret experiments designed to measure D. In some cases, experimental observations are inconsistent with predictions from this simple model, which may be due to factors such as the neglect of moving boundaries, convective mass transport, or non-equilibrium conditions at interfaces. Alternatively, these observations of so-called anomalous diffusion may be the result of a failure of Fick's law (2).[26–28]

The Deborah number is a useful dimensionless quantity to describe the rheological behavior of viscoelastic fluids.[29–31] This dimensionless group is defined as $De = \tau_p/\tau_F$, where τ_p is a characteristic time for stress relaxation in a polymeric system, and τ_F is a characteristic time for the flow under consideration. In mean-field theories for entangled linear polymers, τ_p is the time required for a polymer chain to diffuse a distance equal to its contour length while constrained by a tube, or slip-links, that represent the presence of other chains.[32] For $De \ll 1$, a viscous fluid response is observed, for $De \gg 1$, the response is elastic, and for $De \sim 1$, the response of the material is viscoelastic.

The Deborah number concept has also been applied to diffusion in polymer systems[33] defining $De_D = \tau_p/\tau_D$ as the diffusion Deborah number, where $\tau_D = L^2/D$ is a characteristic time for a diffusion process, and L is a characteristic length. For systems with $De_D \sim 1$, viscoelastic diffusion is anticipated where diffusive transport is coupled to the relaxation of polymer chains. In such cases, Fick's law (2) is no longer valid and the diffusive mass flux depends on the time evolution of the concentration field.[34,35] The strong dependence of both τ_p and D on concentration make systematic experimental studies of viscoelastic diffusion a challenge. In addition, since D for polymer systems can be quite small, the practical range of L is limited.

In the present study, we examine the diffusion of a molecular probe in several polymer melts using Forced Rayleigh Scattering. Using this optical technique, we are able to measure the diffusion coefficient D of a dye over a length scale that can be varied by two orders of magnitude so that the time scale for diffusion τ_D is varied by a factor of 10^4. Since only trace amounts of dye are needed, D should be constant and depend only on dye and polymer chemistry. And, since η and τ_p depend only on the polymer chemistry and molecular weight, we are able to systematically evaluate the Stokes–Einstein relation (1) over a wide range of diffusion Deborah numbers De_D. In the next section, we describe the polymer-dye systems and principle of the experimental measurements. This is followed by a presentation and discussion of our results; the final section gives the conclusions of this study.

2 Experimental considerations

2.1 Materials and methods

Experiments were carried out on poly-isobutylene (PIB) and poly-isoprene (PIP) melts with relatively narrow molecular weight distributions (Polymer Source Inc.). The weight-average molecular weight (M_w) and poly-dispersity (M_w/M_n) from the supplier for the three samples considered is given in Table 1. Also given in this table is the average number of entanglements per chain $Z = M_w/M_e$, where M_e is the entanglement molecular weight.[36,37]

For all three materials, small amplitude oscillatory shear experiments were performed using a parallel-plate geometry on a strain-controlled rheometer (RMS 800, Rheometrics, Inc.). These measurements yielded the complex shear modulus $G^* = G' + iG''$ over a range of frequencies ω, where $G'(\omega)$ and $G''(\omega)$ are the storage and loss modulus, respectively. These experiments were performed at several temperatures and, using time-temperature superposition, were shifted to 298 K to obtain the master curves shown in Fig. 1. These results are typical for well-entangled ($Z \gg 1$) linear polymer melts. The behavior observed in Fig. 1 in the terminal region ($G'' > G'$) for the two PIB melts suggest the presence of a high-molecular weight tail, which is consistent with the somewhat larger (compared to the PIP melt) poly-dispersity for these samples. The data in

Table 1 Molecular weight distribution and rheological properties of the polymer melt samples at 298 K[a]

Sample	M_w [kDa]	M_w/M_n	Z^b	η_0 [kPa s]	τ_p [s]
PIB81k	81	1.18	12	360 ± 40	2.0 ± 0.2
PIB131k	131	1.24	20	890 ± 90	10 ± 1
PIP145k	145	1.03	23	45 ± 5	0.32 ± 0.03

[a] PIB131k shift factor at 323 K is 0.128. [b] $Z = M_w/M_e$; M_e (PIB) = 6.7 kDa; M_e (PIP) = 6.4 kDa.[36,37]

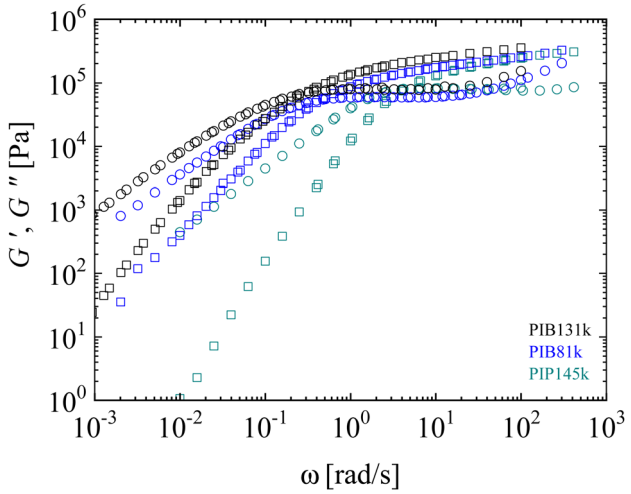

Fig. 1 Shear storage G' (squares) and loss G'' (circles) moduli *versus* frequency ω for PIB131k (black), PIB81k (blue) and PIP145k (green) at 298 K.

Fig. 1 were used to estimate the zero-shear viscosity η_0 and mean relaxation time τ_p that are reported in Table 1.

Here, we investigate the diffusion of a dye in the PIB and PIP polymer melts using an optical technique described below. An ideal dye for such measurements is the fulgide dye known as Aberchrome 540 (AB540, Aberchromics Limited UK), which undergoes a light-induced, reversible conversion between different isomers having different optical properties.[38] As shown in Fig. 2, exposure to ultra-violet (UV) radiation causes the bleached (colorless) isomer of AB540 to undergo a con-rotatory ring closure converting it to the colored (red-orange) isomer. The colored form is reversibly converted back to the bleached isomer by exposure to radiation in the visible (VIS) spectrum. Both isomers are thermally stable up to 100 °C,[20,38] and have diffusivities that are similar.[24] The effective radius R of AB540 is estimated to be 0.38 nm,[39] which relative to the tube diameter $a \approx 6$ nm for both PIB and PIP polymers, gives $2R/a \approx 0.1$.

Samples where prepared by first dissolving AB540 in cyclohexane. Next, polymer was added to the solution such that the weight percent of dye relative to the polymer was 0.025%, or 0.05%, and subjected to gentle mixing for several days. The resulting solution having polymer concentration ~10% by mass was passed through 5 μm and 0.5 μm Teflon filters into a shallow Petrie dish. The solvent was removed in a two-step process: (i) the bulk of the solvent evaporated at atmospheric conditions for several days; (ii) the remaining solvent was removed by placing the semi-dry polymer film in a vacuum oven for several weeks. The entire process took 3–4 weeks and was carried out at room temperature taking care to prevent dust from contaminating the sample. Small amplitude oscillatory tests were performed on the dried, dye-containing polymers and no difference in G^* was detected between these results and those obtained on the as-received materials (see Fig. 1).

The optical technique for performing diffusion measurements relies on the dye having the proper photochemical behavior, which was characterized using a UV-VIS-NIR spectrometer (PerkinElmer, Lambda 19). As shown in Fig. 3, an initially bleached PIB131k-AB540 sample ($t_{exp} = 0$) has an absorption coefficient of $K \approx 0$ in the visible part of the spectrum $\lambda \approx 400$–750 nm. The results for exposing the bleached sample to UV radiation (Spectroline ENF-240C) with wavelength 360 nm and intensity 0.9 mW cm^{-2} for different exposure times t_{exp} are shown in Fig. 3. From this figure we see that as the exposure time t_{exp} is increased, the absorption coefficient K increases for wavelengths in the range $\lambda \approx 450$–550 nm, while $K \approx 0$ for $\lambda > 550$ nm, so that the sample has a red-orange color. For the optical technique described below, the absorption coefficient should be in the range $K = 10$–20 cm^{-1} for $\lambda = 514.5$ nm, which is achieved for exposure times 500–1000 s. The photochemical behavior of AB540 was qualitatively the same in both PIB and PIP melts.

As noted above, the colored form of AB540 can be converted to the bleached isomer by exposure to visible light. This is the basis of the optical technique described below, where the sample is subjected to a short, high-intensity, pulse of duration t_p causing a decrease in the concentration of colored isomers, and hence change in absorption coefficient $\Delta K = K(0) - K(t_p)$. An example of this is shown in Fig. 4 for the case when a PIB131k with 0.025% AB540 sample and $K(0) = 20$ cm^{-1} is subjected to a laser pulse $t_p = 20$ ms with wavelength 514.5 nm

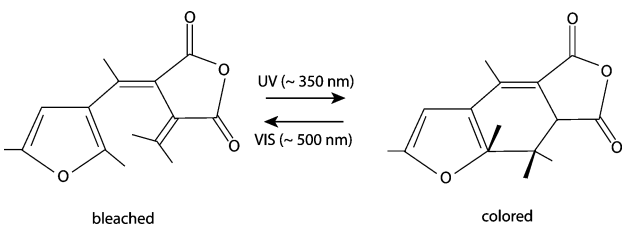

Fig. 2 Photoisomerism of Aberchrome 540 (AB540) showing bleached (left) and colored (right) isomers and approximate wavelengths of radiation to induce reversible isomerism.

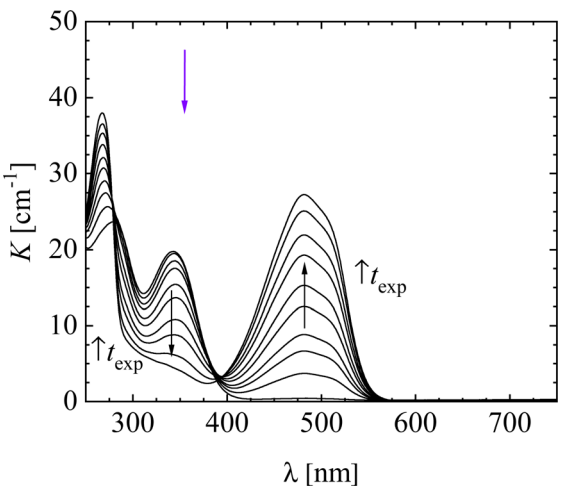

Fig. 3 Absorption coefficient K as a function of wavelength λ for PIB131k-AB540 (0.025%) sample for different exposure times to UV radiation (purple arrow) of wavelength 360 nm: $t_{exp} = 0$, 30, 60, 90, 150, 210, 330, 450, 690, 1050, 1410 s.

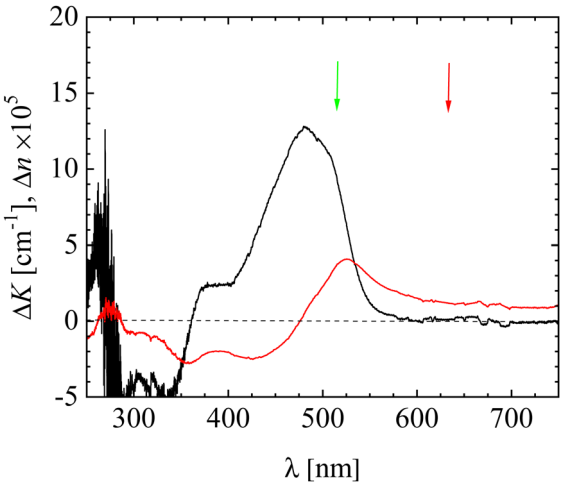

Fig. 4 Change in absorption coefficient ΔK (black curve) as a function of wavelength λ for bleaching a PIB131k-AB540 (0.025%) sample with initial K = 20 cm^{-1} by exposure to radiation of wavelength 514.5 nm (green arrow) for a pulse time t_p = 20 ms. The corresponding change in refractive index Δn (red curve) was computed using the Kramers–Kronig relation. The red arrow corresponds to wavelength 633 nm.

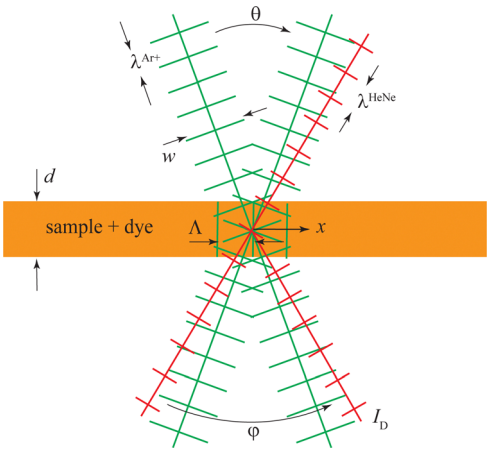

Fig. 5 Schematic of Forced Rayleigh Scattering (FRS) technique showing the intersection of the writing beams (green) within the sample to form a grating with wavelength Λ, and the reading beam (red) passing through the grating resulting in a diffracted beam with intensity I_D.

and intensity 0.8 W cm^{-2}. Similar tests with different laser pulse times t_p and radiation intensities indicate the bleaching reaction follows first-order kinetics,[40] which confirms the absence of any chemical interactions between the dye and polymer. The refractive index n and absorption coefficient K are the real and imaginary parts, respectively, of the complex (frequency-dependent) complex refractive index. As such, n and K are related through the Kramers–Kronig relation.[41] Fig. 4 shows the refractive index change Δn computed from ΔK. We note that $\Delta n \sim 10^{-5}$ for $\lambda \approx$ 550–750 nm while $\Delta K \approx 0$.

2.2 Forced Rayleigh scattering

We employ the technique known as Forced Rayleigh Scattering,[19] which sometimes is referred to as holographic grating relaxation, to study the diffusion of a dye probe in several polymer melts. In our lab, we have used FRS to measure thermal diffusivity (conductivity) in isotropic polymers,[42,43] and to investigate deformation-induced anisotropic thermal conduction in polymer melts subjected to step and constant rate shear flows,[44–48] cross-linked elastomers subjected to uniaxial elongation,[49–52] and in polymers quenched after uniaxial elongation in the melt state.[53–55]

The FRS technique is shown schematically in Fig. 5. The first step of FRS is the creation (writing) of an optical grating by the intersection of two coherent laser beams with wavelength λ^{Ar+} = 514.5 nm and diameter $w \approx$ 3.5 mm. The interference of the beams produces a sinusoidal intensity modulation in the x-direction with grating period $\Lambda = \lambda^{Ar+}/2\sin\theta$, where θ is the angle at which they intersect. We note that our FRS experiments were designed such that the requirements for the plane grating approximation[19,42] were satisfied: $\lambda^{Ar+}/w \ll 1$, $\theta d/4w \ll 1$ and $Kd < 1$, where d = 0.5,1.0 mm is the sample thickness. In our experimental setup, we are able to achieve a wide range of grating sizes Λ from 0.5–70 μm. As shown in Fig. 5, the dyed sample is placed in the interference zone. Absorption of the modulated radiation at wavelength λ^{Ar+} = 514.5 by the uniformly distributed dye (AB540) results in the photochemical conversion of the dye from its colored to bleached isomer (see Fig. 2). Hence, a square writing pulse of duration t_p creates a sinusoidal modulation of the concentrations of the two isomers described by

$$\rho_A(x, t) = \langle \rho_A \rangle + \delta\rho_A(t)\cos(2\pi x/\Lambda) \quad (4)$$

where $\langle \rho_A \rangle$ is the average concentration and $\delta\rho_A(t)$ is the amplitude of the concentration modulation. Since $\Lambda/w \ll 1$, the dynamics of the average concentration are decoupled from the dynamics of $\delta\rho_A$ so that substitution of (4) in (3) and taking D to be constant leads to

$$\delta\rho_A(t) = \delta\rho_A(0)\exp(-t/\tau_D) \quad (5)$$

where $\delta\rho_A(0)$ is the initial amplitude of the modulation (following a pulse of duration t_p), and τ_D is the characteristic time for diffusion, or grating relaxation time, given by

$$\tau_D = \frac{\Lambda^2}{4\pi^2 D}. \quad (6)$$

From (6) we see that measurements of grating relaxation time τ_D for a given grating period Λ allow for the determination of the diffusion coefficient D of the dye AB540 in a polymer melt.

The second step of the FRS technique is detection (reading) of the optical grating. The optical grating formed in the first step is due to the sinusoidal modulation of the concentration of the two isomers of AB540, which have different optical properties. Recall that for $\lambda > 550$ nm, both AB540 isomers do not absorb ($K \approx 0$) (see Fig. 3), while changes in the concentration of the isomers lead to a change in refractive index (see Fig. 4). We exploit this using a reading laser (see Fig. 5) with wavelength λ^{HeNe} = 633 nm to detect the optical 'phase' grating where $\Delta n \propto \delta\rho_A$.[19] Hence, the reading beam is not absorbed by the sample so that no photo-induced isomerism

occurs and the concentration of the AB540 isomers evolves as a result of diffusion alone.[20–23,25]

Our experiments satisfy the thick grating criterion:[19] $d/\Lambda \gg 1$, and we consider first-order Bragg diffraction with the reading beam passing through the grating at angle $\phi/2 = \lambda^{HeNe}/2\Lambda$ (see Fig. 5). The intensity I_D of the reading beam diffracted by the phase grating follows $I_D \propto (\Delta n)^2$, which means that $I_D \propto \exp(-2t/\tau_D)$. In addition to I_D, coherently and incoherently scattered light with intensities I_C and I_E, respectively, which are caused by dust and scratches in the sample, are also read by the photo-detector. For the homodyne detection setup used here, the total intensity striking the photo-detector is given by:[19]

$$I = I_D + 2\sqrt{I_C I_D}\cos\psi + I_C + I_E, \quad (7)$$

where ψ is the (unknown) phase angle between I_C and I_D. Hence, the voltage output of the photo-detector can be expressed as

$$V(t) = A\exp(-2t/\tau_D) + B\exp(-t/\tau_D) + C, \quad (8)$$

where A, B, and C are constants. After obtaining C from the average voltage for $t \gg \tau_D$, A, B and τ_D are determined using a Levenberg–Marquardt algorithm as described elsewhere.[42] We also employed the regularization algorithm known as CONTIN[56] to fit the voltage decay to an arbitrary sum of exponentials, which resulted in two terms having time constants separated by a factor of approximately two consistent with the expression in (8).

The FRS setup employed here is similar to the one used in our previous studies of thermal transport in polymers[42–55] with several important differences. In these previous studies, the thermal grating relaxation time $\tau_T \sim 10^{-3}$ s is many orders of magnitude smaller than τ_D. In this study, we cover a much wider range of grating periods Λ, and pulses of the writing beam (Innova 90C-5) of duration t_p = 10, 20 ms are generated with a mechanical shutter. Also, since $\tau_D \approx 10$–10^4 s, a portion of the reading beam (JDS Uniphase 1125) was split off before the sample and measured to normalize the intensity of the scattered signal so that fluctuations and/or drift in the incident beam were removed. The intensity of both the diffracted and reference beams was measured using silicone photodiode receivers (New Focus 2001). Measurements on all three polymer melts were conducted at 298 ± 1 K; for PIB131k measurements were also conducted at 323 ± 1 K.

Representative examples of the decay of the photo-detector voltage are shown in Fig. 6. In both examples, the fit of (8) to the measured voltage appears to be good. These two examples show the extremes in the quality of the fitting procedure as evident from the distribution of residuals with Fig. 6a showing Gaussian distribution of residuals while Fig. 6b shows that the residuals deviate somewhat from a Gaussian distribution. Fits for both PIB and PIB systems over the range of grating periods investigated fall within this range in terms of fit quality.

3 Results and discussion

We have measured the grating relaxation time τ_D over a wide range of grating periods Λ using the FRS technique for two PIB and one PIP polymer melts with the dye AB540. Recall that changing Λ only requires changing the intersection angle of the writing beams. The results of these measurements are shown in Fig. 7. Included are tests with two pulse times t_p = 10, 20 ms for several grating sizes and no dependence on t_p was observed. From this figure, we see that τ_D has a quadratic dependence on Λ as required by (6). The consistency of the results for the PIB81k and PIB131k systems indicate that the diffusion coefficient is independent of polymer chain length. This suggests diffusion of the molecular probe is decoupled from chain relaxation and is consistent with theoretical predictions for nanoparticle-polymer systems[12] for well-entangled polymer melts. Furthermore, the temperature dependence observed for the PIB131k results 298 K and 323 K indicate a decrease in the effect of friction (increase in D) on diffusive transport with increasing temperature. Similar observations have been reported for nanoparticle–polymer

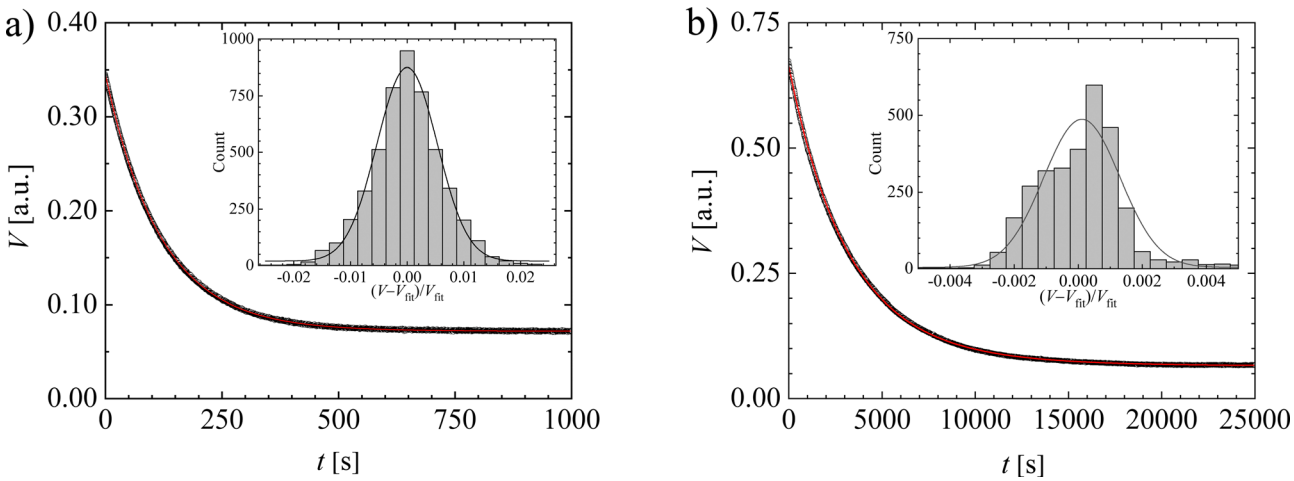

Fig. 6 Examples of normalized photo-detector voltage (○) *versus* time for PIB131k-AB540 at 298 K with pulse time t_p = 20 ms: (a) grating size Λ = 10.5 μm; (b) grating size Λ = 49.4 μm. In each plot, the solid red curve in represents the fit to eqn (8). The insets show the distribution of residuals from fit with a Gaussian distribution (black curve) having the same mean and standard deviation of the residuals.

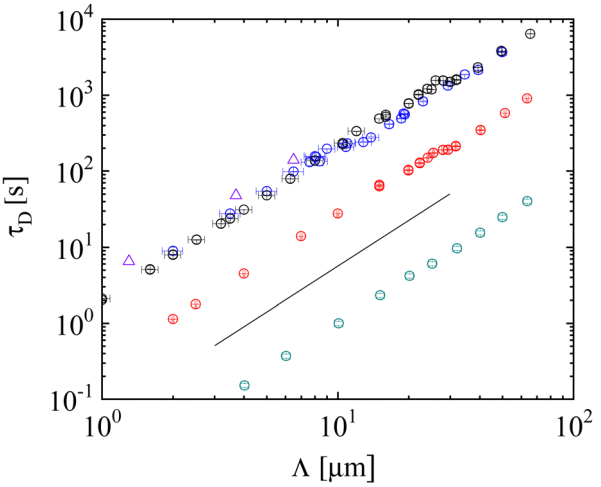

Fig. 7 Grating relaxation time *versus* grating period Λ for diffusion of AB540 dye from FRS measurements on PIB81k (○), PIB131k (○), PIP145k (○) at 298 K, and PIB131k at 323 K (○). Also shown are FRAP data[18] for the diffusion of rubrene dye in PIB85k at 312 K (△). The solid line has a slope of 2.

systems.[7,9] Also shown in Fig. 7 are results for the diffusion of the dye rubrene in a broad molecular weight distribution PIB melt (M_w = 85 kDa) measured at 312 K with FRAP.[18] One would expect τ_D for this system to fall between the results for PIB131k at 298 K and PIB131k at 323 K in Fig. 7. The larger values of τ_D (smaller D) suggest the rubrene probe has a larger size compared to the AB540 dye used in the present study.

Closer inspection of Fig. 7 reveals for several systems an apparent jump where τ_D has a given value for multiple values for Λ. These jumps are observed for PIB81k (298 K) and PIB131k (298 K & 323 K), but not for PIP145k (298 K). It is important to note that the quality of the fits to the photodetector voltage for grating periods Λ near the jump were qualitatively similar to those shown in Fig. 6. Deviations from $\tau_D \propto \Lambda^2$ have been reported for diffusion in latex films,[22,23,25]

Table 2 Summary of measured diffusion coefficient D for AB540 in different polymer melts obtained from the slopes of the lines in Fig. 8. τ_D^* is the estimated value of the diffusion time scale where the change in D occurs

Polymer	T [K]	D [μm^2 s^{-1}]	τ_D^* [s]	D [μm^2 s^{-1}]
PIB81k	298	0.011 ± 0.002	200 ± 25	0.017 ± 0.002
PIB131k	298	0.012 ± 0.001	1500 ± 200	0.017 ± 0.002
PIB131k	323	0.097 ± 0.001	200 ± 25	0.110 ± 0.001
PIP145k	298	2.58 ± 0.02		

which is expected given the heterogeneous nature of these systems. Similar results have also been obtained for the diffusion of nanoparticles in agarose solutions.[15] To our knowledge, the results in Fig. 7 appear to be the first reports of anomalous diffusion of a molecular probe in polymer melts.

A clearer picture of these jumps can be seen in Fig. 8 where Λ^2 is plotted *versus* τ_D. The non-linear dependence of Λ^2 on τ_D is an indication non-Fickian diffusion; however, there are two regimes where the diffusion appears to be Fickian. According to (6), the slope of the solid lines equals $4\pi^2 D$, which indicate an increase in D passing through the jump. These results, which are presented in Table 2, indicate changes in D ranging from 14–55%. Also included in this table are rough estimates for the grating relaxation time τ_D^* where the change in the value of D occurs. Values for the diffusion coefficient D of AB540 in PIB and PIP melts in Table 2 measured using FRS are consistent with those obtained for the diffusion of different molecular probes in well-entangled polymer melts using FRAP[18] and FCS[13] techniques.

In Fig. 9 the measured diffusion coefficient D normalized by the Stokes–Einstein prediction (1) is plotted as a function of the diffusion Deborah number $De_D = \tau_p/\tau_D$. From this figure it is evident that the diffusion coefficient is from four to five orders of magnitude larger than the continuum prediction of the Stokes–Einstein equation. This behavior can be explained by the small size of the probe (AB540) relative to the tube diameter

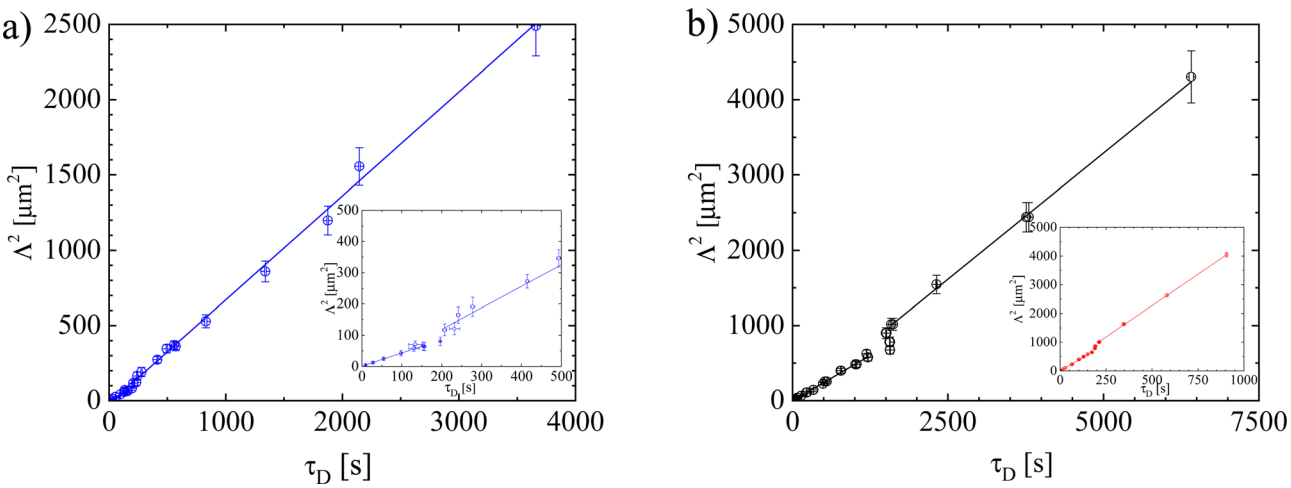

Fig. 8 Square of the grating period Λ *versus* grating relaxation time τ_D obtained from results in Fig. 7 (note symbol colors). (a) PIB81k at 298 K (inset shows magnified view of slope change); (b) PIB131k at 298 K (inset shows results at 323 K). Solid lines are linear fits to data before and after change in diffusivity (slope).

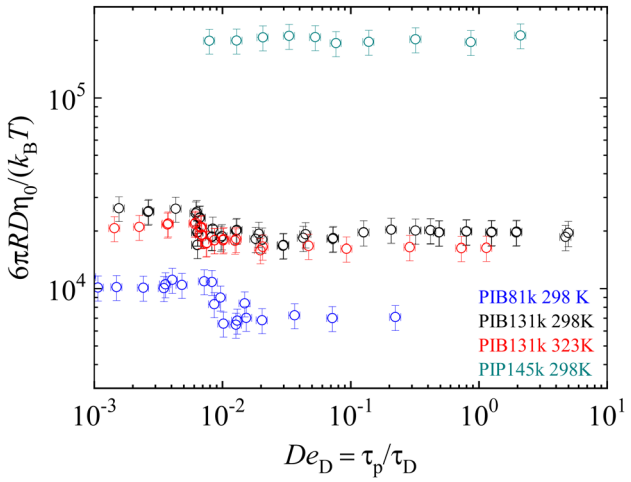

Fig. 9 Diffusion coefficient D normalized by the Stokes–Einstein prediction (1) for AB540 dye diffusion in PIB81k (○), PIB131k (○), PIP145k (○) at 298 K, and PIB131k at 323 K (○).

of the polymer chain $2R/a \ll 1$, and is consistent with both experiments and predictions for the diffusion of nanoparticles in polymer melts.[7–12] The collapse of results for PIB131k at 298 K & 323 K indicates that the reduced local friction on the probe causes an increase in the diffusion coefficient D as well as a decrease in polymer viscosity η_0 such that $\eta_0 D/T$ is approximately constant over this small temperature range. Similarly, the results for PIB81k fall below those for the PIB131k since the local friction experienced by the probe is independent of polymer chain length, while the viscosity η_0 is not. The results for rubrene diffusion in PIB shown in Fig. 7 would show a deviation of more than three orders of magnitude from (1); this has been explained in terms of rotational correlation time for the probe.[18] The PIP141k results in Fig. 9 indicate the diffusion coefficient for probe is roughly 200 000 times larger than the Stokes–Einstein prediction (1). We further note that the results in Fig. 9 do not show evidence of deviations from Ficks' law (2), which one might expect for $De_D \sim 1$. It is possible that viscoelastic diffusion is observed only for polymer–solvent systems where the mutual diffusion process results in the perturbation of polymer chain configurations.[33]

The jumps in D observed in Fig. 7 and 8 for PIB81k (298 K) and PIB131k (298 K & 323 K) are also evident in Fig. 9. Interestingly, the jumps in the normalized diffusion coefficient shown in Fig. 9 occur for values of the Deborah number for diffusion $De_D = \tau_p/\tau_D \approx 10^{-2}$. One explanation for this somewhat surprising result is diffusion by a hopping mechanism,[57–59] which has been suggested for the diffusion of nanoparticles in polymer solutions and gels. An alternative explanation is based on the so-called constraint release mechanism,[60–62] which alters the dynamics of polymer chain diffusion along its contour length. The tube, or slip links, that constrain the motion of a polymer chain along its contour length are the result of other chains, which themselves are moving along their own contour lengths. Hence, constraint release, which is sometimes referred to as tube dilation, has the effect of enlarging the confining tube of a given polymer chain. The relaxation time for constraint release is given by $\tau_{CR} = Z^2\tau_p$. Estimates for τ_{CR} obtained using the values of Z and τ_p in Table 1 yield values for τ_{CR} that are within a factor of roughly three of the estimated values of τ_D^* in Table 2. Given this semi-quantitative agreement, it seems reasonable to suggest that the jump in D occurs for $\tau_{CR}/\tau_D \sim 1$, and the increase in D is observed when $\tau_D \gtrsim \tau_{CR}$. Assuming the constraint release mechanism leads to an increase in the effective tube diameter, this would have the effect of decreasing the ratio of probe size to tube diameter $2R/a$. Indeed, theoretical models for diffusion in nanoparticle–polymer systems predict a dramatic increase in D with decreasing $2R/a$ for $2R/a \lesssim 1$.[11,12] This picture is also consistent with the absence of a jump in D for PIP141k, which would require grating relaxation times $\tau_D \sim 10^2$ s or larger, or grating periods $\Lambda \sim 10^2$ μm, which can not be achieved with our FRS setup.

4 Conclusions

We have measured the diffusion coefficient of a molecular probe, the dye Aberchrome 540, in several entangled polymer melts using the optical technique known as forced Rayleigh scattering (FRS). These measurements were performed on polymers with relatively narrow molecular weight distributions under the condition that the probe size was much smaller than the tube diameter, that is $2R/a \ll 1$. Standard linear viscoelastic measurements on these polymers were used to obtain the zero-shear rate viscosity η_0 and polymer relaxation time τ_p. The unique optical properties of the dye allowed for straightforward interpretation of the FRS experiments, and for the determination of the grating relaxation time τ_D for a wide range of grating periods Λ.

The dependence of τ_D on Λ was quadratic as anticipated. However, an unexpected jump was observed for three sets of data on polyisobutylene (PIB) melts such that the value of the diffusion coefficient D changed by up to 50% at a particular value of τ_D. Observation of this anomalous, or non-Fickian, diffusion was made possible by covering a range of diffusion time scales τ_D that varied by nearly four decades. This phenomenon was not observed in measurements on a polyisoprene (PIP) melt. The measured diffusion coefficients D for both PIB and PIP melts are from four to five orders of magnitude larger than the prediction of the Stokes–Einstein relation. This result is similar to those found both experimentally and theoretically for the diffusion of nanoparticles in polymer melts and is attributed to the viscous drag force exerted on the probe being significantly smaller than the bulk viscosity of polymer. Furthermore, we found no evidence of viscoelastic diffusion over a wide range of diffusion Deborah number $De_D = \tau_p/\tau_D$.

Finally, we have made a connection between the change in diffusion coefficient and the constraint release mechanism that can be important to polymer chain dynamics. Constraint release leads to an increase in the tube diameter and, hence, a decrease in the relative size of the probe $2R/a$. We argue that the observed increase in diffusion coefficient occurs for diffusion times that are larger than the relaxation time for constraint release τ_{CR},

that is for $\tau_D \gtrsim \tau_{CR}$. This hypothesis is consistent with estimates for τ_{CR} for the polymer melts considered in this investigation. Hence, while the diffusive motion of small probes in entangled polymers is decoupled from the dynamics of the entire chain, it appears that the constraint release mechanism can have an appreciable effect on the local environment experienced by the probe.

Author contributions

DCV conceived of and directed this study. VR, SS and DNS conducted all experiments and performed data analysis. DNS and DCV wrote the first draft manuscript, which was revised by all authors before submission.

Conflicts of interest

There are no conflicts to declare.

Acknowledgements

The authors gratefully acknowledge partial support for this study provided by the ACS Petroleum Research Fund grant No. 36659-AC9. The authors also thank Professor Timothy P. Lodge for providing the AB540 dye used in this study and Professor Jay D. Schieber for useful discussions.

Notes and references

1 P. Neogi, *Diffusion in Polymers*, Marecel Dekker Inc., New York, 1996.
2 C. C. Miller, *Proc. Roy. Soc. A*, 1924, **106**, 724–749.
3 D. Ehlich and H. Sillescu, *Macromol.*, 1990, **23**, 1600–1610.
4 C. T. Thurau and M. D. Ediger, *J. Chem. Phys.*, 2003, **118**, 1996–2004.
5 A. Karatrantos, R. J. Composto, K. I. Winey, M. Kröger and N. Clarke, *Polymers*, 2019, **11**, 11050876.
6 E. J. Bailey and K. I. Winey, *Prog. Polym. Sci.*, 2020, **105**, 101242.
7 A. Tuteja, M. E. Mackay, S. N. S. Asokan and M. S. Wong, *Nano Lett.*, 2007, **7**, 1276–1281.
8 C. A. Grabowski, B. Adhikary and A. Mukhopadhyay, *Appl. Phys. Lett.*, 2009, **94**, 021903.
9 C. A. Grabowski and A. Mukhopadhyay, *Macromol.*, 2014, **47**, 7238–7242.
10 R. Mangal, S. Srivastava, S. Narayanan and L. A. Archer, *Langmuir*, 2016, **32**, 596–603.
11 F. Brochard and P. G. de Gennes, *Eur. Phys. J. E: Soft Matter Biol. Phys.*, 2000, **1**, 93–97.
12 U. Yamamoto and K. S. Schweizer, *Macromol.*, 2015, **48**, 152–163.
13 T. Cherdhirankorn, V. Harmandaris, A. Juhari, P. Voudouris, G. Fytas, K. Kremer and K. Koynov, *Macromol.*, 2009, **42**, 4858–4866.
14 D. Wöll, *RSC Adv.*, 2014, **4**, 2447–2465.
15 D. S. Banks, C. Tressler, R. D. Peters, F. Höfling and C. Fradin, *Soft Matter*, 2016, **12**, 4190–4203.
16 M. Antonietti, D. Ehlich, H. Sillescu and M. Wesselmann, *Prog. Colloid Polym. Sci.*, 1989, **80**, 83–92.
17 M. T. Cicerone, F. R. Blackburn and M. D. Ediger, *Macromol.*, 1995, **28**, 8224–8232.
18 D. Bainbridge and M. D. Ediger, *Rheol. Acta*, 1997, **36**, 209–216.
19 H. J. Eichler, P. Gunter and D. W. Pohl, *Laser-Induced Dynamic Gratings*, Springer-Verlag, Berlin, 1986.
20 T. S. Frick, W. J. Huang, M. Tirrel and T. P. Lodge, *J. Polym. Sci., Part B: Polym. Phys.*, 1990, **28**, 2629–2649.
21 G. Heuberger and H. Sillescu, *J. Phys. C: Solid State Phys*, 1996, **100**, 15225–15260.
22 E. Bartsch, T. Jahr, A. Veniaminov and H. Sillescu, *J. Phys. IV France*, 2000, **10**, Pr7-289–Pr7-293.
23 A. Veniaminov, T. Jahr, H. Sillescu and E. Bartsch, *Macromol.*, 2002, **35**, 808–819.
24 A. Veniaminov, T. Eckert, H. Sillescu and E. Bartsch, *Macromol.*, 2003, **36**, 4944–4953.
25 K. I. Suresh, A. Veniaminov and E. Bartsch, *J. Polym. Sci., Part B: Polym. Phys.*, 2007, **45**, 2823–2834.
26 J. S. Vrentas, J. L. Duda and A. C. Hou, *J. Appl. Polym. Sci.*, 1984, **29**, 399–406.
27 P. Neogi, *AIChE J.*, 1986, **29**, 829–832.
28 C. J. Durning and M. Tabor, *Macromol.*, 1986, **19**, 2220–2232.
29 M. Reiner, *Phys. Today*, 1964, **17**, 62.
30 A. Metzner, J. L. White and M. M. Denn, *AIChE J.*, 1966, **12**, 863–866.
31 G. Marrucci and G. Astarita, *Meccanica*, 1967, **2**, 141–143.
32 M. Doi and S. F. Edwards, *The Theory of Polymer Dynamics*, Oxford University Press, Oxford, 1986.
33 J. S. Vrentas, C. M. Jarzebski and J. L. Duda, *AIChE J.*, 1975, **21**, 894–901.
34 G. Camera-Roda and G. C. Sarti, *AIChE J.*, 1990, **36**, 851–860.
35 D. Jou, J. Casas-Vázquez and G. Lebon, *Rep. Prog. Phys.*, 1998, **62**, 1035–1142.
36 L. J. Fetters, D. J. Lohse and R. H. Colby, *J. Polym. Sci., Part B: Polym. Phys.*, 1999, **37**, 1023–1033.
37 M. Rubinstein and R. H. Colby, *Polymer Physics*, Oxford University Press, New York, 2003.
38 H. G. Heller and J. R. Langan, *J. Chem. Soc. Perkin Trans. II*, 1981, 341–343.
39 G. Heuberger and H. Sillescu, *J. Phys. C: Solid State Phys.*, 1996, **100**, 15255–15260.
40 M. Rappon, A. Chuenarm, A. J. Duggal, H. Gill, O. Bhaovibul and R. T. Syvitski, *Eur. Polym. J.*, 1991, **27**, 365–370.
41 J. D. Jackson, *Classical Electrodynamics*, Wiley, New York, 2nd edn, 1975.
42 D. C. Venerus, J. D. Schieber, H. Iddir, J. D. Guzmán and A. W. Broerman, *J. Polym. Sci., Polym. Phys. Ed.*, 1999, **37**, 1069–1078.
43 A. Kiessling, D. Nieto Simavilla, G. G. Vogiatzis and D. C. Venerus, *Polymer*, 2021, **228**, 123881.
44 D. C. Venerus, J. D. Schieber, H. Iddir, J. D. Guzmán and A. W. Broerman, *Phys. Rev. Lett.*, 1999, **82**, 366–369.

45 D. C. Venerus, J. D. Schieber, H. Iddir, J. D. Guzmán and A. W. Broerman, *Int. J. Thermophys.*, 2001, **22**, 1215–1225.
46 D. C. Venerus, J. D. Schieber, V. Balasubramanian, K. Bush and S. Smoukov, *Phys. Rev. Lett.*, 2004, **93**, 098301.
47 J. D. Schieber, D. C. Venerus, K. Bush, V. Balasubramanian and S. Smoukov, *Proc. Natl. Acad. Sci. U. S. A.*, 2004, **101**, 13142–13146.
48 V. Balasubramanian, K. Bush, S. Smoukov, D. C. Venerus and J. D. Schieber, *Macromol.*, 2005, **38**, 6210–6215.
49 A. W. Broerman, D. C. Venerus and J. D. Schieber, *J. Chem. Phys.*, 1999, **111**, 6965–6969.
50 D. C. Venerus and D. N. Kolev, *Macromol.*, 2009, **42**, 2594–2598.
51 D. Nieto Simavilla, J. D. Schieber and D. C. Venerus, *J. Polym. Sci., Part B: Polym. Phys.*, 2012, **50**, 1638–1644.
52 D. C. Venerus, D. Nieto Simavilla and J. D. Schieber, *Rubber Chem. Tech.*, 2019, **92**, 639–652.
53 J. D. Schieber, D. C. Venerus and S. Gupta, *Soft Matter*, 2012, **8**, 11781–11785.
54 S. Gupta, J. D. Schieber and D. C. Venerus, *J. Rheol.*, 2013, **57**, 427–439.
55 D. C. Venerus and A. Agarwal, *J. Polym. Sci., Part B: Polym. Phys.*, 2019, **57**, 547–553.
56 S. W. Provencher, *Comput. Phys. Commun.*, 1982, **27**, 229–242.
57 L.-H. Cai, S. Panyukov and M. Rubinstein, *Macromol.*, 2015, **48**, 847–862.
58 J. Ramirez, T. J. Dursch and B. D. Olsen, *Macromol.*, 2018, **51**, 2517–2525.
59 K. K. Senanayake, A. Ehsan Akbari Fakhrabadi, M. W. Liberatore and A. Mukhopadhyay, *Macromol.*, 2019, **52**, 787–795.
60 W. W. Graessley, *Advances in Polymer Science*, 1982, pp. 67–117.
61 J. L. Viovy, *J. Phys.*, 1985, **45**, 847–853.
62 J. des Cloizeaux, *Europhys. Lett.*, 1988, **5**, 437–442.

